AIP | Journal of Applied Physics

Optical and electrical properties of gold nanowires synthesized by electrochemical deposition

Huijun Yao, Jinglai Duan, Dan Mo, Hacı Yusuf Günel, Yonghui Chen et al.

Citation: J. Appl. Phys. **110**, 094301 (2011); doi: 10.1063/1.3656733
View online: http://dx.doi.org/10.1063/1.3656733
View Table of Contents: http://jap.aip.org/resource/1/JAPIAU/v110/i9
Published by the American Institute of Physics.

Optical and electrical properties of gold nanowires synthesized by electrochemical deposition

Huijun Yao,[1,2,a)] Jinglai Duan,[1] Dan Mo,[1] Hacı Yusuf Günel,[2] Yonghui Chen,[1] Jie Liu,[1] and Thomas Schäpers[2]
[1]*Institute of Modern Physics, Chinese Academy of Sciences, Lanzhou 730000, People's Republic of China*
[2]*Peter Grünberg Institute (PGI-9) and JARA-FIT Jülich-Aachen Research Alliance, Forschungszentrum Jülich GmbH, D-52425 Jülich, Germany*

(Received 15 June 2011; accepted 24 September 2011; published online 2 November 2011)

Gold nanowire arrays with different sizes were fabricated by electrochemical deposition in etched ion-track templates. The diameter of the gold nanowires between 30 and 130 nm could be well adjusted by pore sizes in the templates through etching time. Single-crystalline nanowires were achieved by changing the parameters of electrochemical deposition. The morphology and crystal structure of the fabricated gold nanowires were characterized by means of scanning electron microscopy and transmission electron microscopy. The optical properties of the gold nanowire arrays embodied in templates were systematically measured by absorption spectra with a UV/Vis/NIR spectrophotometer. Due to the surface plasmon resonance effect, the extinction peaks of gold nanowire arrays possessed a red-shift with increasing wires diameter and a blue-shift with decreasing angle between incident light and nanowire arrays. The failure current density of the single gold nanowire as a function of diameter was determined and the failure mechanism was also discussed. © *2011 American Institute of Physics*. [doi:10.1063/1.3656733]

I. INTRODUCTION

Nanowires, unlike other low-dimensional systems, have two quantum-confined directions but one unconfined direction available for electrical conduction. At the same time, owing to their unique density of electronic states, in the limit of small diameters, nanowires are expected to exhibit significant different optical, electrical, and magnetic properties than their bulk 3-D crystalline counterparts. Nanowires may become important building blocks for nanoscaled electronics, e.g., sensors,[1,2] optical switching,[3] and detectors.[4,5] Significantly, the ability to assemble and electrically drive nanoscale sources and detector blocks could allow for fully integrated nanophotonic systems for the applications ranging from biodetection through information processing.

As an important research field, interaction between light and metal nanowires has attracted much attention through its applications to nonlinear optics,[6] surface enhanced Raman scattering,[7] and plasmonics.[8] These nanowire systems strongly absorb incident light at specific frequencies of surface plasmon resonances (SPR). Although the optical properties of metal spheres have already been described by Mie's theory in 1908,[9] the relationship between the nanowire's geometries and their nonlinear optical properties has not been fully investigated.[10–12] Hence, the production of metal nanowires with controllable size, geometry, and distribution is important to theoretical research and technological applications utilizing surface plasmon resonance.

The metal nanowires are of considerable interest to nanoelectronics and future super large-scale integration circuits because of their potential use as interconnects, sensors, or integral device components. The electrical properties of metal nanowires, such as resistivity, failure current density, and joule heating effect, are regarded as essential factors to evaluate metal nanowires for future applications. Although it is well-known that as the dimensions of metal nanowires shrink, the resistivity and failure current density increase due to increased scattering of the conduction electrons by the surface of the nanowires, internal grain boundaries, and surface-to-volume ratio.[13,14] The key issue for nanotechnology is how significantly this increased scattering affects the electrical properties of single nanowire.

Etched ion-track template method has been proved to be a well established method for producing metal and semiconductor nanowires by filling the pores with aimed materials.[13–15] The ease and low cost of the process means it is very attractive option for industrial applications. Preparing nanowires in the etched ion-track template with electrodeposition has the advantage that the nanowires can be grown with large aspect ratios and vertical alignment on a substrate. Furthermore, the density of the nanowire in the template can be adjusted easily by varying the fluence of the irradiating ions. We have previously reported the gold,[15] copper,[11] cobalt,[16] CdS,[10] and polypyrrole nanowires[17] deposited into ion-track templates.

The metal gold, as a universal noble metal, is a suitable material to study SPR properties and electrical transport properties, because of its prominent confinement in the charge carriers and stabilization in physical and chemical properties. We report on the successful fabrication of gold nanowire arrays with controlled size and crystallinity in ion-track templates by electrochemical method. We focus our attention on the SPR properties of gold nanowire arrays and the electrical properties of single gold nanowires.

[a)]Author to whom correspondence should be addressed. Electronic mail: yaohuijun@impcas.ac.cn.

II. EXPERIMENT

The 30 μm polycarbonate membranes (Makrofol N, Bayer Leverkusen) were irradiated at the UNILAC linear accelerator of GSI (Darmstadt, Germany) with Au ions (kinetic energy 11.4 MeV/u, fluence 1×10^8 ions/cm^2) in normal incidence. After irradiation, each side of the membrane was exposed to UV light for 2 h, in order to enhance the ratio of track etching rate over bulk etching rate. This step guarantees that the etched pores are with fine cylindrical shapes in the next etching process. The membranes were etched in 5 M/l NaOH solution at 50 °C for 1 to 5 min to obtain ion-track templates with nanopores ranging from 30 to 130 nm. During etching process, an ultrasonic field was employed to achieve homogeneous pore etching. A thin gold film was sputtered onto one side of the membrane and reinforced electrochemically with a copper layer in tens of microns as a substrate. This layer served later as a conducting substrate cathode and a platinum wire as an anode during the electrodeposition of gold nanowires in the pores. In this process, the employed electrolyte was $Na_3Au(SO_3)_2$ (concentration = 0.1 M/l) and the applied voltage was chosen as 1.5 V. The growth process of gold nanowires was monitored through recording the deposition current versus time curves. After that, the membrane was dissolved by dichloromethane (CH_2Cl_2) while the gold nanowires were still attached on the copper substrate. The morphology and the size of the deposited gold nanowires were investigated by scanning electron microscopy (SEM; JSM 6701 and 5600LV) and transmission electron microscopy (TEM; JEOL 3010). The optical properties of gold nanowire arrays embedded in ion-track templates after removing the copper substrate were studied by using a UV/Vis/NIR spectrophotometer (Lambda 900, Perkin-Elmer).

To characterize and analyze the electron transport properties, the gold nanowires were mechanically transferred from the original copper substrate to a highly conductive Si (100) wafer coated with a 100 nm thick SiO_2 insulating layer. This host substrate was patterned in advance with contact pads and markers. The markers were used to determine the exact position of the randomly disposed wires for the following electron beam lithography step. In order to get good Ohmic contacts between the contact electrodes and nanowires, oxygen plasma was used to remove the contamination on the surface of gold nanowires. Finally, the wires were contacted individually with non-annealed Ti/Au electrodes patterned by electron beam lithography.[18]

III. RESULTS AND DISCUSSION

After ion-track template being dissolved, the gold nanowires on the copper substrate are imaged by SEM. The typical SEM images of gold nanowires with the diameter of 100 nm are presented in Fig. 1. As shown in Fig. 1(a), apparently a great number of nanowires with tens of micrometers in length are collapsed on the copper substrate and aggregate together. This phenomenon can be attributed to high aspect ratio of nanowires, and the surface tension of solvent drops while drying the sample in the process of template dissolution.[10,19] As can be seen with high-magnification SEM image

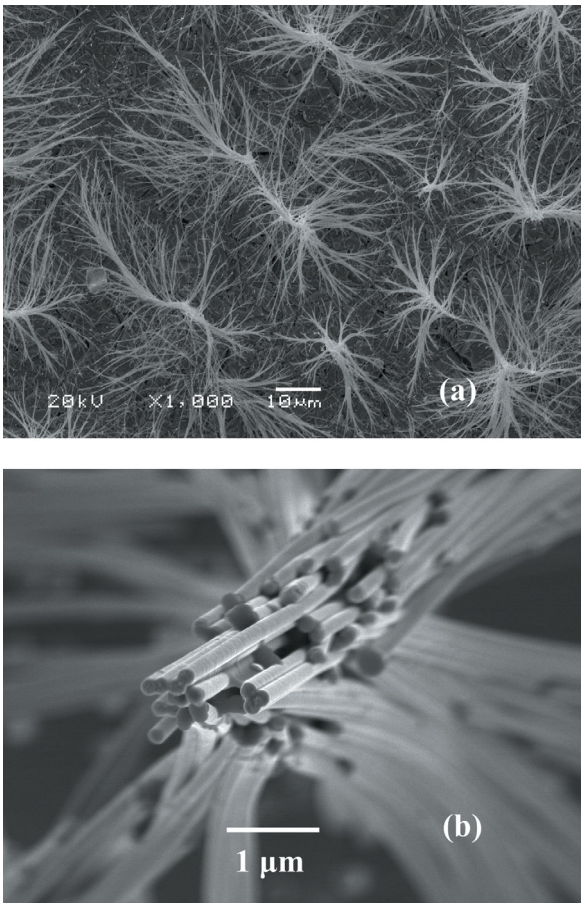

FIG. 1. (Color online) SEM images of gold nanowires of 100 nm in diameter observed with (a) low magnification and (b) high magnification.

in Fig. 1(b), the surface of gold nanowires with 100 nm in diameter is very smooth.

As evidenced by TEM in Fig. 2(a), the wires with the diameter of around 53 nm possess cylindrical shape with smooth and homogeneous contours. Thanks to the good quality of the etched ion-track templates, the diameter distribution within a given sample is also very narrow. The single crystal-structure of gold nanowires is confirmed using selected area electron diffraction (SAED), as depicted in Fig. 2(b).

To investigate the optical properties, the extinction spectra of gold nanowire arrays were measured by transmission method after removing substrate layers of gold and copper from the template. The gold nanowire arrays were still embedded in the ion-track template as displayed in Fig. 3 when their optical properties were investigated. Due to the normal irradiating polycarbonate membrane with parallelized heavy ions from accelerator, the gold nanowires deposited in the later porous template are highly parallel to each other without connection and overlap, which is beneficial to investigating optical properties of gold nanowire arrays. The extinction spectra of gold nanowire arrays with different diameters are represented in Fig. 4 as the propagation direction of incident light is parallel to the long axis of the wire (Z-axis). It shows that the extinction peak caused by gold nanowire arrays appears at 511 nm when the diameter of gold nanowires is 30 nm, while it shifts to longer wavelength

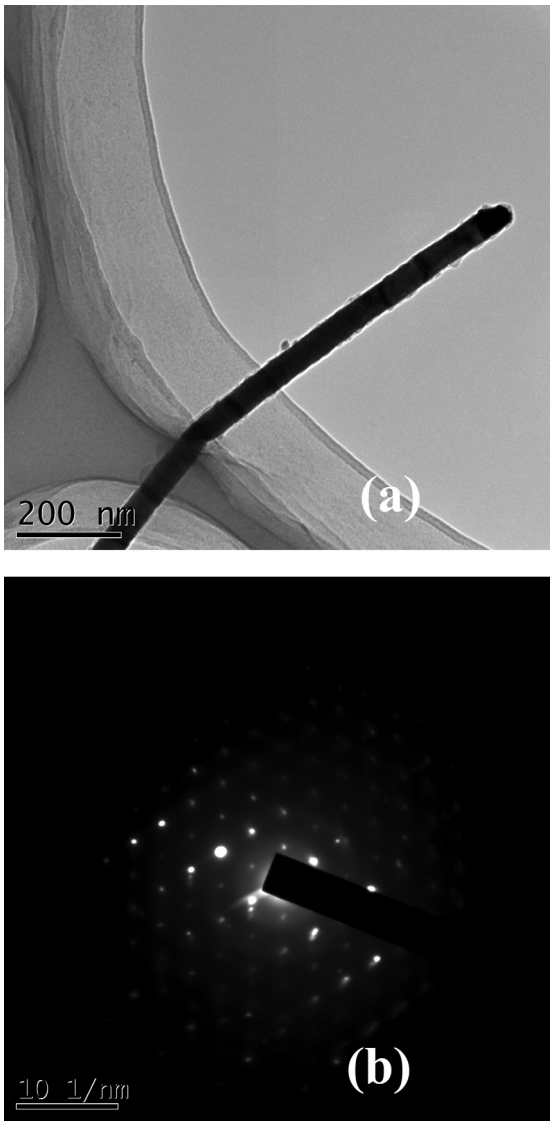

FIG. 2. (a) TEM image of a 53 nm gold nanowire with obvious uniform contour and (b) SAED pattern of the gold nanowire shown in (a).

with increasing diameter. For the wires with diameter of 130 nm, the extinction peak shifts to 596 nm.

The absorbance of nano-scale metal materials to incident light can be assigned to so-called SPR,[20,21] which is the collective oscillation of the free conduction electrons at the surface driven by an external electromagnetic field of incident light. The excited collective electron oscillations within the particles then radiate electromagnetic waves of the same frequency into the far field[22] or convert into other forms of energy such as heat.[23] The SPR is very sensitive to the kind, size, shape, crystal structure, and dielectric constant of the metal and surrounding medium (here: polycarbonate).[8,21,24–27] In the case of Fig. 4, as schematically illustrated by Fig. 3(a), at normal (0°) incidence, the electric fields of P-polarized and S-polarized component included in the incident light are along the two short axes (X-axis and Y-axis) of the nanowires; thus, only the transverse resonances are excited by the short axes of the gold nanowires,[27–29] while the electric field along the long axis (Z-axis) of the nanowires is not excited.[30] This is the key difference to the nanowires or nanorods in

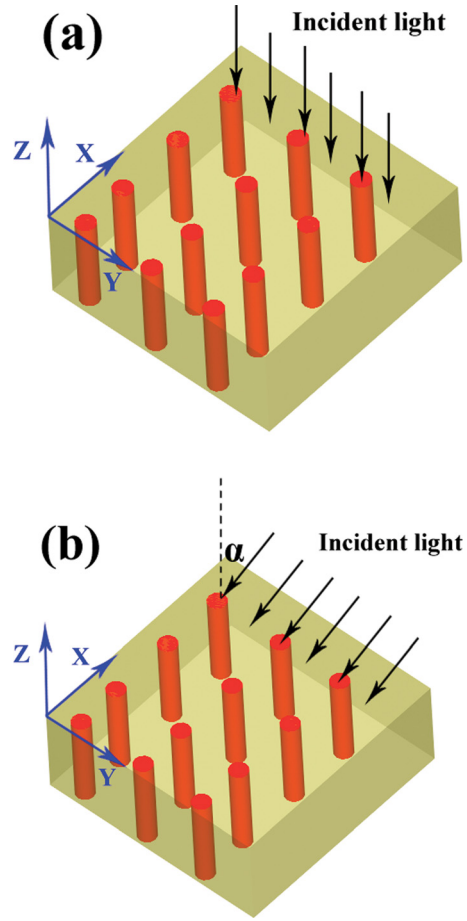

FIG. 3. (Color online) The schematic description of two different modes for investigating the optical properties. The gold nanowires embodied in the etched ion-track template are highly parallel to each other. α is the angle between propagation direction of inject light and long axes of nanowires, (a) $\alpha = 0°$ and (b) $0° < \alpha < 90°$; the X and Y axes are along the short axes of the gold nanowires, and Z-axis is parallel to the long axis.

solution or dispersed horizontally on a substrate. In our case, there are two possible reasons for extinction peak red shifting with increasing the diameter of nanowires. One possible reason is the size effect. From the top view of Figure 3(a), the

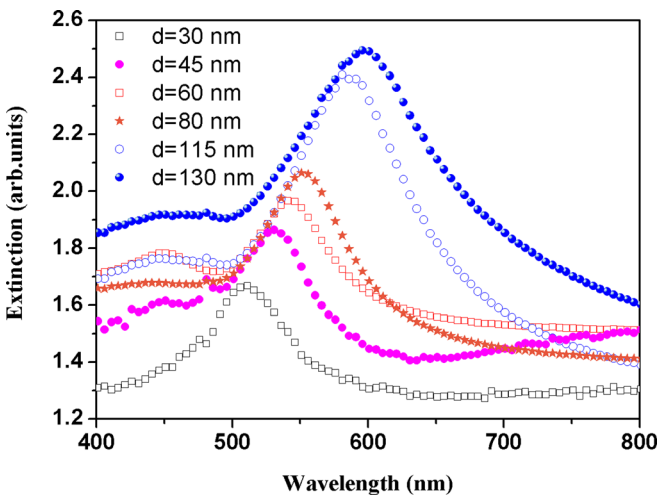

FIG. 4. (Color online) Extinction spectra of gold nanowire arrays with the diameters from 30 to 130 nm. The area density of the gold nanowires measured here is 1×10^8 wires/cm^2.

nanowire arrays can be treated as distributed nanoplates or nanospheres because only transverse resonances can be excited as we discussed previously. Under this assumption, the extinction peak will shift to longer wavelength with increasing the size of nanoplates or nanospheres,[31] which is equivalent to the diameter of nanowires. Another possible reason for the extinction peak changing is enhanced coupling effect among the nanowires. The propagation distance and degree of confinement of the plasmon guided modes depend strongly on the separation between wires. Individual wire modes are recovered at large separations, while mode hybridization is observed when the spacing is reduced.[32] Previous studies have demonstrated that, in an array of nanorods, the SPR of the individual nanorods can be viewed as harmonic oscillators that couple to each other, leading to a resonance shift as well as a changed near-field distribution.[33] In the present work, the mean distances between the wire surfaces facing each other decreases from 470 to 370 nm with the nanowires diameters increasing from 30 to 130 nm at the certain area density of 1×10^8 wires/cm^2 (with the assumption of all nanopores in the templates being filled).[34] It is reported that if the distance of the nanowires or nanorods surfaces is around or smaller than 2.5 times the diameter, the coupling among the nanowires or nanorods results in a red shift of the transverse plasmon.[35] For the nanowires with high aspect ratio (length/diameter), this effect could also be easily observed even when the distance between nanowires was larger than 15 times the diameter as shown in our experiments (cf. Fig. 4). The observed peak broadening can be ascribed to the polydispersity in the nanowires distance and overlap of the gap mode with the metal.[32]

The absorbance properties of gold nanowire arrays with different incident angle α were also investigated [Fig. 3(b)]. In case of $\alpha > 0°$, according to the previous discussion, there will be an electric field of P-polarized component along the long axis (Z-axis) of gold nanowires and the longitudinal resonance should be excited. However, it should be noted that the Gans theory[36] for gold nanowires with aspect ratio larger than 20 predicts a longitudinal peak in the infra-red, rather than in the visible, which is beyond our spectra range. The extinction peak of 80 nm gold nanowire arrays is shifted from 552 to 529 nm with incident angle α increasing from 0° to 50° as shown in Fig. 5. In case of other diameters, the extinction peaks shift to shorter wavelength with increasing incident angle α in the same way. The blue-shift of the SPR peak with increasing incident angle is mainly caused by the phase delay of the incident light due to the array.[33] It is known that the strongest coupling occurs when the linked electric fields are in phase. With increasing angle α, the coupling-effect between the neighboring wires is expected to decrease because of the increasing phase difference of incident electric field. Therefore, the coupling strength is lowered and, consequently, the resonance peak shifts to shorter wavelengths.

To characterize the electrical properties of single gold nanowire, Ti/Au electrodes were patterned onto a gold nanowire. In Fig. 6(a), a SEM image of typical two-terminal measurement structure is shown. The gold nanowire with a diameter of 85 nm is connected by two metal contacts separated by 924 nm.

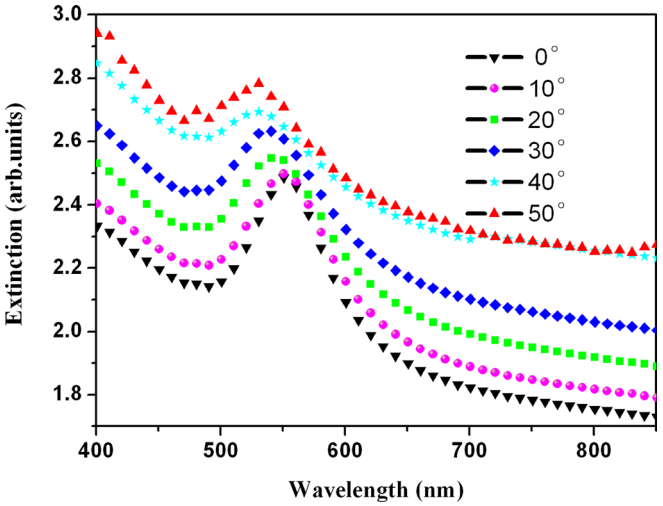

FIG. 5. (Color online) Extinction spectra of 80 nm gold nanowires with different incidence angles α. The area density of gold nanowire measured is 1×10^8 wires/cm^2.

By increasing the applied voltage between the two electrodes, the current density increased until a rupture of the wire occurred. A typical I-V measurement curve is shown in Fig. 7(a). The measured current increases linearly for small voltage and become nonlinear for bias voltage larger than 0.25 V. This nonlinear increase can be attributed to the positive temperature coefficient of the resistivity for gold.[37,38] Due to Joule heating, the mean temperature of the gold

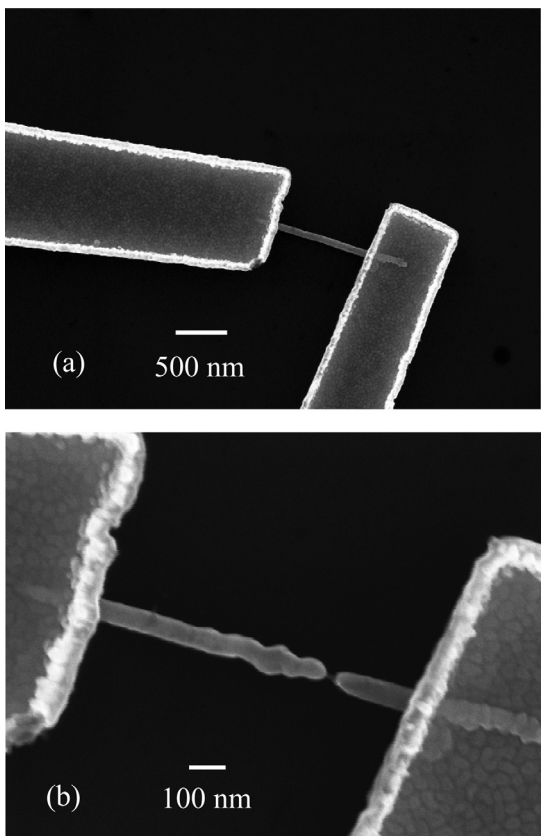

FIG. 6. SEM images of a single gold nanowire for measuring the failure current density. (a) Before performing the measurement; (b) disrupted gold nanowire by a high current density.

nanowire increases with higher currents and so does the resistivity.[14] In Fig. 7(a), after the maximum current of 9.15 mA appearing, the current drops to zero and I-V curve forms a circular bead in stead of a sharp angle in the break point, which indicates the breakdown process. Fig. 6(b) shows the SEM image of the broken gold nanowire after undergoing the failure current testing. A bamboo structure is found in the broken gold nanowire and the breaking happens in the "neck" area of the bamboo. There are two possible reasons for this phenomenon. One possible reason for the appearance of bamboo structure during failure current measurement is the existence of "hot spots" within gold nanowire, i.e., localized points of higher resistance than the surrounding materials due to grain boundaries, impurities, or defects.[14,39] There will be more momentum transfer from the electrons to the ions which makes up the hot spots of the wire.[13,40] These hot spots locally have more Joule heating and thus localize higher temperatures which in turn increase the resistivity thus forming a feedback for increased Joule heating. When the melting point in a hot spot is reached, the bamboo structure begins to appear because of uneven thermal stress along gold nanowire. Another possible reason is the grain restructuring in the gold nanowire. The grain restructuring will be driven by the thermal activation of the grains as well as by the high local electric fields due to the presence of grain boundaries. As the temperature being highest at the center of gold nanowire, the gathering of grains and thermal stress will be formed there.[41] The temperature profile leads to more rapid growth of grains at the center of the wire than at the ends, thus making it probable that the center of the wire has a bamboo structure. Based on the above analysis, the main mechanisms for gold nanowire going breakdown are melting, which is caused by high current density and an uneven thermal stress. For the existence of "hot spots" or grain restructuring during measuring, the temperature increasing along the gold wire is inhomogeneous. That is the reason why we did not estimate the temperature prior to melt according to $\Delta T = \Delta R/\alpha R_0$, where α (diameter dependent[38]) is the linear temperature coefficient of the resistance for gold nanowires, although a resistance increasing can be confirmed at higher current during the measurement as shown in Fig. 7(a). In addition, the average pre-melting temperature calculated from this model would be much lower than the real melting temperature in the broken area of the wire.

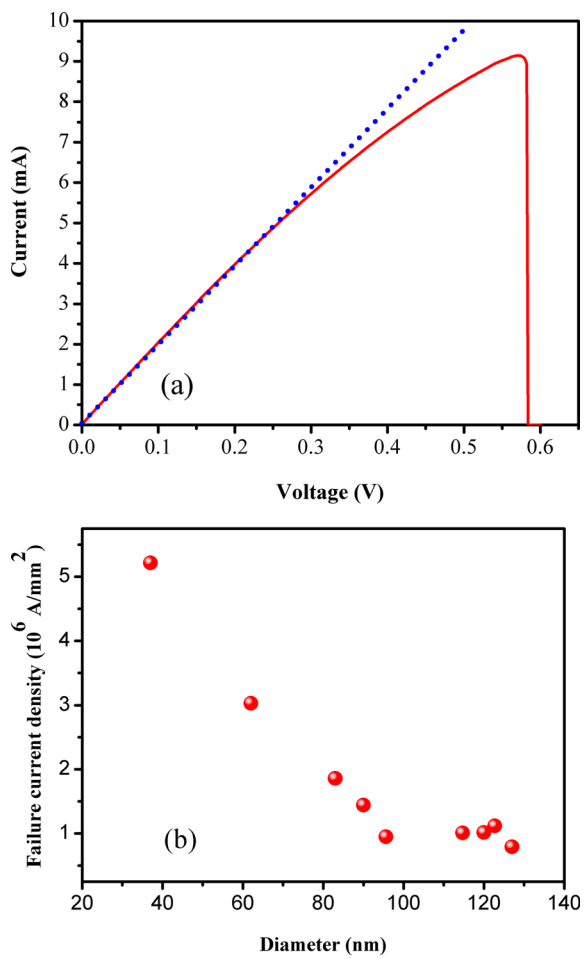

FIG. 7. (Color online) (a) The record I-V curve of single gold nanowire for measuring maximum current density, the dotted line is used to guide the eye; (b) failure current density of single gold nanowires as a function of diameter.

The failure current density, i.e., the ratio of failure current over the cross-section area of the wire, was calculated by performing I-V measurement as shown in Fig. 7(a). In Fig. 7(b), the failure current density of single gold nanowires is plotted as a function of diameter. The failure current density around 1.0×10^6 A/mm^2 increases slowly with the nanowires diameter d in the range of 95–130 nm. When the diameter $d < 95$ nm, the failure current density increases faster with decreasing diameter and reaches a maximum value of 5.2×10^6 A/mm^2 in case of $d = 37$ nm in our experiments. The thermal radiation, which will be influenced by the exposed surface-to-volume ratio, can be negligible because there is not enough time for radiating heat to surrounding in the seconds measuring period. In our measurements, most of the heat transfer occurs at the interface of nanowire and SiO_2 substrate, where the substrate acts as a heat sink.[14] The smaller size of the nanowires allows a large percentage of the gold atoms to be positioned at the surface of a nanowire and these surface atoms are more responsive to heat diffusion. At the same time, the electron scattering from the wire surface is no longer negligible.[37] The heat transfer efficiency would increase with the decreasing nanowire's size, i.e., increasing of surface-to-volume ratio, and so failure current density does.

IV. CONCLUSIONS

Gold nanowire arrays with the diameters from 30 to 130 nm were successfully fabricated by electrochemical deposition in ion-track templates and the single crystal structure of gold nanowires was confirmed by TEM. The optical extinction properties of gold nanowire arrays embedded in the etched ion-track templates were studied. It is proved that the transverse resonance peak moved to longer wavelengths with gold nanowire diameter, increasing for size effect and enhanced coupling among nanowires. The relationship between the gold nanowire arrays' extinction spectra and incident angle of the inject light was also studied. It is inferred that the spectra peak shifted to shorter wavelengths

with the angle increasing which is mainly caused by weakening couple effect among wires for the phase retardation. In addition, I-V failure measurements indicated that the gold nanowires comparing to its bulk counterpart exhibited a higher failure current density as the diameter decreased because of the increased surface-to-volume ratio and higher heat transfer efficiency from the nanowire to substrate. Meanwhile, for the failure mechanism of single gold nanowire, the melting and uneven thermal stress contribute to it together.

ACKNOWLEDGMENTS

One of the authors (H.J.Y.) would like to thank the Chinese Academy of Sciences (CAS) for research scholarships as visiting scientist at Forschungszentrum Jülich, Germany. The authors gratefully acknowledge the finance support from the West Light project of the Chinese Academy of Sciences, National Natural Science Foundation of China (Grant Nos. 11005134, 10805062, and 10975164), and the Natural Science Foundation of Gansu Province (1007RJYA014) and thank the Materials Research Department of GSI (Darmstadt, Germany) for the performing of ion irradiation experiments on polycarbonate membrane, H. P. Bochem for SEM, and Dr. Trellenkamp for electron beam writing.

[1]E. C. Walter, R. M. Penner, H. Liu, K. H. Ng, M. P. Zach, and F. Favier, Surf. Interface Anal. **34**, 409 (2002).
[2]R. MacKenzie, C. Fraschina, T. Sannomiya, V. Auzelyte, and J. Voros, Sensors **10**, 9808 (2010).
[3]X. P. Zhang, B. Q. Sun, J. M. Hodgkiss, and R. H. Friend, Adv. Mater. **20**, 4455 (2008).
[4]J. Kong, N. R. Franklin, C. W. Zhou, M. G. Chapline, S. Peng, K. J. Cho, and H. J. Dai, Science **287**, 622 (2000).
[5]F. Hernandez-Ramirez, S. Barth, A. Tarancon, O. Casals, E. Pellicer, J. Rodriguez, A. Romano-Rodriguez, J. R. Morante, and S. Mathur, Nanotechnology **18**, 424016 (2007).
[6]T. Kitahara, A. Sugawara, H. Sano, and G. Mizutani, Appl. Surf. Sci. **219**, 271 (2003).
[7]Z. Q. Tian, B. Ren, and D. Y. Wu, J. Phys. Chem. B **106**, 9463 (2002).
[8]W. L. Barnes, A. Dereux, and T. W. Ebbesen, Nature **424**, 824 (2003).
[9]G. Mie, Ann. Phys. **25**, 377 (1908).
[10]D. Mo, J. Liu, H. J. Yao, J. L. Duan, M. D. Hou, Y. M. Sun, Y. F. Chen, Z. H. Xue, and L. Zhang, J. Cryst. Growth **310**, 612 (2008).
[11]J. L. Duan, J. Liu, H. J. Yao, D. Mo, M. D. Hou, Y. M. Sun, Y. F. Chen, and L. Zhang, Mater. Sci. Eng., B **147**, 57 (2008).
[12]R. L. Zong, J. Zhou, B. Li, M. Fu, S. K. Shi, and L. T. Li, J. Chem. Phys. **123**, 094710 (2005).
[13]Y. Peng, T. Cullis, and B. Inkson, Appl. Phys. Lett. **93**, 183112 (2008).
[14]Q. J. Huang, C. M. Lilley, M. Bode, and R. Divan, J. Appl. Phys. **104**, 023709 (2008).
[15]J. Liu, J. Duan, E. Toimil-Molares, S. Karim, T. W. Cornelius, D. Dobrev, H. Yao, Y. Sun, M. Hou, D. Mo, Z. Wang, and R. Neumann, Nanotechnology **17**, 1922 (2006).
[16]J. Duan, J. Liu, T. W. Cornelius, H. Yao, D. Mo, Y. Chen, L. Zhang, Y. Sun, M. Hou, C. Trautmann, and R. Neumann, Nucl. Instrum. Methods Phys. Res. B **267**, 2567 (2009).
[17]Y. F. Chen, J. Liu, H. J. Yao, D. Mo, J. L. Duan, M. D. Hou, Y. M. Sun, L. Zhang, and K. Maaz, Physica B **405**, 2461 (2010).
[18]C. Blömers, Th. Schäpers, T. Richter, R. Calarco, H. Lüth, and M. Marso, Phys. Rev. B **77**, 201301 (2008).
[19]Y. T. Pang, G. W. Meng, Y. Zhang, Q. Fang, and L. D. Zhang, Appl. Phys. A **76**, 533 (2003).
[20]A. Henglein, J. Phys. Chem. **97**, 5457 (1993).
[21]A. Henglein, Chem. Rev. **89**, 1861 (1989).
[22]K. H. Su, Q. H. Wei, X. Zhang, J. J. Mock, D. R. Smith, and S. Schultz, Nano Lett. **3**, 1087 (2003).
[23]M. I. Mishchenko, L. D. Travis, and A. A. Lacis, *Scattering, Absorption, and Emission of Light by Small Particles* (Cambridge University Press, Cambridge, 2002).
[24]H. Ditlbacher, A. Hohenau, D. Wagner, U. Kreibig, M. Rogers, F. Hofer, F. R. Aussenegg, and J. R. Krenn, Phys. Rev. Lett. **95**, 257403 (2005).
[25]J. Mock, M. Barbic, D. Smith, D. Schultz, and S. Schultz, J. Chem. Phys. **116**, 6755 (2002).
[26]P. R. Evans, G. A. Wurtz, R. Atkinson, W. Hendren, D. O'Connor, W. Dickson, R. J. Pollard, and A. V. Zayats, J. Phys. Chem. C **111**, 12522 (2007).
[27]P. R. Evans, W. R. Hendren, R. Atkinson, and R. J. Pollard, Nanotechnology **19**, 465708 (2008).
[28]S. Kim, K. L. Shuford, H. M. Bok, S. K. Kim, and S. Park, Nano Lett. **8**, 800 (2008).
[29]S. Y. Yim, H. G. Ahn, K. C. Je, M. Choi, C. W. Park, H. Ju, and S. H. Park, Opt. Express **15**, 10282 (2007).
[30]P. R. Evans, R. Kullock, W. R. Hendren, R. Atkinson, R. J. Pollard, and L. M. Eng, Adv. Funct. Mater. **18**, 1075 (2008).
[31]P. K. Jain, K. S. Lee, I. H. El-Sayed, and M. A. El-Sayed, J. Phys. Chem. B **110**, 7238 (2006).
[32]A. Manjavacas and F. J. G. de Abajo, Nano Lett. **9**, 1285 (2009).
[33]R. Kullock, W. R. Hendren, A. Hille, S. Grafstrom, P. R. Evans, R. J. Pollard, R. Atkinson, and L. M. Eng, Opt. Express **16**, 21671 (2008).
[34]J. L. Duan, T. W. Cornelius, J. Liu, S. Karim, H. J. Yao, O. Picht, M. Rauber, S. Muller, and R. Neumann, J. Phys. Chem. C **113**, 13583 (2009).
[35]A. M. Funston, C. Novo, T. J. Davis, and P. Mulvaney, Nano Lett. **9**, 1651 (2009).
[36]R. Gans, Ann. Phys. **4**, 270 (1915).
[37]S. Karim, W. Ensinger, T. W. Cornelius, and R. Neumann, Physica E **40**, 3173 (2008).
[38]Q. J. Huang, C. M. Lilley, R. Divan, and M. Bode, IEEE Trans. Nanotechnol. **7**, 688 (2008).
[39]T. H. Kim, X. G. Zhang, D. M. Nicholson, B. M. Evans, N. S. Kulkarni, B. Radhakrishnan, E. A. Kenik, and A. P. Li, Nano Lett. **10**, 3096 (2010).
[40]M. Wilms, J. Conrad, K. Vasilev, M. Kreiter, and G. Wegner, Appl. Surf. Sci. **238**, 490 (2004).
[41]C. Durkan and M. E. Welland, Ultramicroscopy **82**, 125 (2000).